2012

Electronic Detection of Ultra Cold Neutral Plasma

Nirakar Poudel
Colby College

Colby College

Honors Thesis

Electronic Detection of Ultra Cold Neutral Plasma

Author:
Nirakar Poudel

Supervisor:
Professor Duncan A. Tate

June 19, 2012

Acknowledgements

First and foremost, I want to express my sincere gratitude to Professor Duncan Tate for all his support, continual encouragement and insights. Without his initial encouragement and support during the difficult time of this project, I would not have been able to write a thesis and hence fulfill my goal of completing a honors major in Physics. Its because of Professor Tate that I have developed a deep appreciation for experimental Physics as well as developed a deeper understanding of Ultra Cold Neutral Plasmas.

Colby Physics department has been extremely helpful to me throughout my time at Colby College. The combination of great professors and inspiring, passionate and dedicated fellow class mates has always motivated me to work hard and provided me the best educational experience I could have ever imagined.

I am extremely thankful to my parents. I want to dedicate this thesis to them. Although far way from here, my parents have always been there to encourage me and support me. Without them, I could have never made it to this point in college.

I am thankful to my dean Sue McDougal for her support during last four years at Colby. She has always encouraged me and instilled faith in me. Colby's international community has been a great support during my college career. Lastly, I would like to thank my very close friends Arjumand Masood, Chiran Singh Bhandari, Rahul Khakurel, Suman Koirala, Utsha Karki, Rijosh Shrestha, Ujwal Sapkota, Anup Dhamala, Aasish Raj Joshi and Srish Khakurel. These guys have always been there for me when have I needed them.

Abstract

The project was started with an objective to investigate the effect of radio frequency absorption in Ultra Cold Neutral Plasmas (UNPs). The plasma oscillation is density dependent and can be excited by using external radio frequency field. A homodyne circuit is used to detect direct absorption of the radio frequency waves. The radio frequency waves are applied to conducting meshes which lie on either side of the plasma. The meshes are effectively a capacitor, which together with inherent circuit resistance constitute a high pass filter. A small part of the gain and phase shift of the filter depend on the presence of the plasma. The gain change and phase change of the initial radio frequency signal by the high pass filter is observed using a digital oscilloscope. The gain change and the phase change signal can be used to identify the resonance point in the ultra cold neutral plasma. The resonant frequency is related to plasma expansion velocity, plasma temperature and plasma density. Therefore, by identifying resonant frequency various plasma parameters can be determined. The results of the experiment were used to identify various modes of plasma oscillations. Due to the limitation of time, only qualitative data analysis was performed. The results are in good qualitative agreement with the theory as well as previous experiments. The data obtained from this project as well as the understanding acquired here can be used in future experiments. In the future, a comprehensive quantitative analysis of the results is necessary to verify the underlying theories as well as accurately determine various plasma parameters.

Contents

List of Figures

1 Introduction

1.1 Plasma

In structured systems like atoms, molecules and crystals, the binding energies are greater than the surrounding thermal energy. When the temperature is greater than the ionization energy, atoms disassociate into electrons and positively charged ions. The positively charged ions and electrons are strongly affected by each other′s electromagnetic fields. However, as the charges are no longer bound to each other, this assembly of positive ions and electrons can demonstrate collective motions of great vigor and complexity. Plasma is the assembly of such electrons and positively charged ions. The Nobel Prize winning American Chemist Irving Langmuir first used the word plasma to describe ionized gases in 1927. Irving Langmuir also laid out the theoretical foundations for all subsequent research in plasma physics.

Although sometimes defined as sufficiently ionized gases capable of demonstrating plasma-like behavior, plasmas are distinct state of matter like solid, liquid and gases. It is often remarked that almost 99% of all matter in the universe is plasma. Plasmas have a big range of density and temperature. We can find plasma of density 10^3 cm^{-3} and temperature of a few hundred kelvin in the aurora of earths ionosphere to a density of 10^{27} cm^{-3} and temperature of 10^7 K in the core of the sun [1]. Terrestrial plasmas are found in fluorescent lamps, lightning, different laboratory experiments and many other industrial processes like integrated circuit fabrication. The sun, stars, solar wind, spaces between planets and galaxies and interstellar nebulae are all made of plasmas.

1.2 Ultra Cold Neutral Plasma

Steve L. Rolston′s research group discovered Ultra Cold Neutral Plasmas (UNPs) in 1999 at NIST [2]. Ultra Cold neutral Plasmas extend the boundaries of the conventional Plasma Physics and provide a new testing ground for exploring new plasma theories. They are formed by photo-ionizing laser-cooled atoms near the ionization threshold and have electron temperatures ranging from 1 to 1000 K and ion temperatures of around 1 K [3]. Ultra cold neutral plasmas can be created in any atomic systems which can be easily laser cooled and which have convenient wavelengths for photoionization. So far they have been created in xenon, rubidium, cesium, strontium and calcium atoms [1].

Two important competing processes take place in a plasma. The electrons and ions in the plasma acquire thermal energy during the ionization process. The positively charged ions create an electrostatic field within the plasma. The electrons are trapped inside the potential well created by the ions. The electrostatic potential tries to hold the electrons within the plasma. Since the electrons also have kinetic energies, they try to escape the electrostatic field. The Coulomb coupling parameter Γ gives the ratio of the electrostatic potential energy to the kinetic energies of the particles. This parameter also measures the strength of inter-particle coupling in plasmas.

$$\Gamma = \frac{e^2}{4\pi\epsilon_0 k_B T} \tag{1.2.1}$$

In equation 1.2.1, T is plasma temperature and $a = \sqrt[3]{\frac{3}{4\pi\rho}}$ is the Wigner-Seitz radius, which is the average separation of the particles in the plasma with density ρ [3]. In UNPs, Γ is greater than or equal to 1, with typical values ranging from 1 to 10^5 [3].

UNPs are excellent medium for studying plasma physics. UNPs have low density

and hence their evolution takes place in a time scale which is experimentally accessible (≈ 10 μs - 1ms). They can be precisely controlled with varying initial conditions and can be reproduced consistently using various experimental techniques. This allows a wide range of high precision experimental measurements to be carried out on UNPs. These kinds of experiments would be very difficult using naturally occurring plasmas. UNPs are excellent medium to test various theoretical predictions of plasma behavior in strongly coupled regimes.

1.2.1 Plasma Creation

Laboratory plasmas are created by photo-ionizing laser cooled atoms in a Magneto Optical Trap (MOT) using pulsed laser. The spatial distribution of the laser cooled atoms, n_a, in a MOT can be modeled by Gaussian function

$$n_a(r) = n_0 \exp(-r^2/2\sigma^2) \tag{1.2.2}$$

where n_0 is the peak density of atoms, σ is the characteristic radius of the atom cloud, ($\approx 300\mu$m) [3]. As many as 10^9 atoms can be cooled to mK or μK temperatures and confined to a density of around 10^{11} cm^{-3} [3]. Right after the photoionization process, a burst of electrons leave the plasma leaving excess positive charge in the plasma. The positively charged ions create a potential well within the plasma and hold the remaining electrons in a self restraining plasma which slowly expands. The plasma forms if the ion density is greater than a threshold value which is determined by the initial electron kinetic energy [4]. Most of the electrons that escape from the plasma are the ones that are on the edges of the plasma. Therefore, the charge imbalance remains on the edges of the plasma while the center of the plasma remains neutral. The plasma is referred to as quasi neutral because of the charge imbalance present

on the edges. The initial electron kinetic energy is given by the equation

$$E_{e,0} \equiv \frac{3}{2} k_B T_{e,0} = h\upsilon - E_{IP} \tag{1.2.3}$$

where $E_{e,0}$, $T_{e,0}$, υ and E_{IP} are the initial electron kinetic energy, initial electron temperature, the ionizing laser frequency and the ionization energy of the atoms in the trap, respectively [4]. Due to the principle of conservation of momentum, most of the excess photon energy is imparted to the electrons because they are much lighter than the positively charged ions. The initial electron kinetic energy and the initial electron temperature are functions of photon energy. The initial electron temperature can be varied from 0.1 to 1000 K by varying the photon energy [4]. The density, potential energy and inter particle spacing in the plasma are all functions of the laser intensity because all these parameters depend on the number electrons ejected from the laser cooled atoms right after photoionization. After the formation of plasma, inelastic collisions between ions and electrons and neutral atoms generate heat in the plasma. The excess energy generated during the collisions is used by the electron cloud to radially expand outwards. As the cloud expands, the density of the positive ions decreases and hence the depth of the potential well also decreases. As a result, more electrons evaporate from the plasma. Almost all the electrons escape from the plasma between 10 to 100 μs. After all the electrons have evaporated, the ions continue to expand, but the plasma is effectively extinguished. The time taken for all the electrons to leave the plasma is referred to as life time of plasma.

Despite the fact that the electrons have been ionized just at the threshold level and have very low excess energy E_e, the electron cloud expands as if the energy is more than E_e. Right after forming, the ions are spatially positioned in a random manner such that there is an excess of potential energy in the system. The ions tend towards

the equilibrium by converting this excess potential energy into thermal energy. This process is referred to as disorder induced heating (DIH) and takes place in a time scale of around 270 ns [3]. In a similar manner, electrons also arrange themselves in order to minimize the potential energy of the system. The time scale for this disorder induced heating takes place in order of tens of mirco seconds in electrons.

Another heating process might take place even before the disorder induced heating takes place. This inelastic process is called three-body recombination (TBR). In this process, two electrons combine with an ion to form a Rydberg atom and an extra electron that absorbs the energy released during the formation of the Rydberg atom. Three-body recombination is a dominating process in ultra-cold plasmas. The rate of three-body recombination varies as $T_e^{-9/2}$ [5].

1.2.2 Theory of Plasma Evolution

The evolution of UNPs on macroscopic level is described by using kinetic and hydrodynamic formulations [3]. In experimental studies, we are interested in the free electrons present in plasmas. Therefore, a simple collision-less hydrodynamic model will be sufficient for our purpose although collisional hydrodynamic model or microscopic model will give a more accurate description of the plasma dynamics. Collision-less hydrodynamic model assumes that the coupling parameters of both the electrons and the ions is less than the unity and neglects any collisional process in the plasma. In this model the distribution of electrons $f_\alpha(r_\alpha, v_\alpha)$ is given by Vlasov equation

$$\frac{\partial f_\alpha}{\partial t} + v_\alpha \frac{\partial f_\alpha}{\partial r_\alpha} - m_\alpha^{-1} \frac{\partial f_\alpha}{\partial v_\alpha} q_\alpha \frac{\partial \varphi\left(r_\alpha\right)}{\partial r_\alpha} = 0 \tag{1.2.4}$$

where $\alpha = e$ for electrons and ions, m_α is the mass of species α, q is the charge of the species α and φ is the mean free potential given by $\nabla^2\varphi = \frac{e}{\epsilon_o}(\rho_e - \rho_i)$. The

spatial electron density distribution, ρ_e, is given as $\rho_e = \int f_\alpha \partial v_\alpha$ [3]. The non-linear equation 1.2.4 does not have any analytical solution. However, a large set of self-similar solutions can be obtained by assuming that the plasma remains quasi neutral throughout its evolution. The solution of particular interest is the case of Gaussian phase space density

$$f_e(\mathbf{r}, \mathbf{v}, t) = \rho_e(\mathbf{r}, t)\phi_e(\mathbf{v}, T_e(t)) \propto \rho_e(\mathbf{r}, t) \exp\left(-\frac{m_e v^2}{2k_B T_e(t)}\right) \tag{1.2.5}$$

where ρ_e is the Gaussian phase space density and ϕ_e is the Maxwell-Boltzmann velocity distribution of the electrons [3]. The expanding plasma in the Magneto-Optical trap retains its shape for all times because of the collision-less and quasi neutral assumptions made in the beginning. Furthermore, the assumption also yields results in which the electron evolution in a plasma can be completely described by the macroscopic parameters σ_e, γ_e and T_e, where σ_e is the root mean squared radius of the Gaussian spatial distribution of the electrons, γ_e is the hydrodynamic electron velocity or the local mean velocity of the electrons and T_e is the temperature of the electrons [3]. Substituting equation 1.2.5 in equation 1.2.4 yields following important results for plasma evolution.

$$\frac{\partial \sigma^2}{\partial t} = 2\gamma_e \sigma^2 \tag{1.2.6}$$

$$\frac{\partial k_B T_e}{\partial t} = -2\gamma_e k_B T_e \tag{1.2.7}$$

Combining these two equations gives a result that $\sigma^2 T_e = Constant$. This result means that that as the plasma expands, the electrons cool adiabatically. Using this important result, analytical solutions for plasma radius σ, electron number density

n_e and the electron temperature T_e can be evaluated.

$$\sigma^2(t) = \sigma^2(0)\left(1 + t^2/\tau_{exp}^2\right) \tag{1.2.8}$$

$$T_e(t) = \frac{T_e(0)}{1 + t^2/\tau_{exp}^2} \tag{1.2.9}$$

$$n(r,t) = \frac{n_0\sigma_0^3}{\sigma^3}\exp(-r^2/2\sigma^2) \tag{1.2.10}$$

In equation 1.2.10, σ_0 is the plasma radius at time $t = 0$ and τ_{exp} is the characteristic time scale of plasma given by

$$\tau_{exp} = \sqrt{m_i\sigma^2(0)/k_B[T_e(0) + T_i(0)]} \tag{1.2.11}$$

Due to the adiabatic expansion, the plasma cools as it expands. The thermal energy of the plasma is transferred to the kinetic energy of the electron cloud. The electron cloud expands due to this kinetic energy. All the analytical solutions are based on the assumptions that the plasma remains quasi-neutral throughout the expansion process. However, during the experiment, an applied voltage removes electrons from the plasma causing charge imbalance in the plasma. The removal of each electron deepens the potential well of the plasma for the remaining electrons. Therefore, the electrons which are near the center of the plasma are strongly bound within plasma. Most of the electrons that get removed by the electric field are on the edges of the plasma. The charge imbalance in plasma can be quantified by the parameter

$$\delta = \frac{N_i - N_e}{N_e} \tag{1.2.12}$$

where N_i and N_e are the initial number of ions and electrons respectively. As the charge imbalance, δ, becomes larger, it affects the plasma behavior and dynamics.

2 Plasma Oscillations and radio frequency response

Plasmas demonstrate different collective modes. Plasma oscillation is one of the most common collective modes and in this mode electrons oscillate around their equilibrium position while the ions are stationary [6]. The measured value of plasma oscillation frequency can be used to find important plasma parameters like plasma expansion velocity, plasma temperature and density. Plasma oscillation can be driven by applying time varying weak external radio frequency field. If this driving frequency equals the plasma oscillating frequency, resonance occurs. The frequency at which the resonance occurs depends on the density of the plasma. When the resonance occurs, the electrons start oscillating faster and some of the energized electrons will acquire enough energy to escape the plasma. These extra electrons ejected from the plasma help us identify the resonance peaks in the electron signal. Three different modes of oscillation have been used to explain the observed resonances in ultra cold neutral plasmas under consideration.

2.1 Local Mode

This mode of plasma oscillation was investigated by Kulin et al. [6]. As the plasma expands, its density decreases. The frequency of the plasma oscillation depends on the density of plasma. Therefore, the plasma oscillation frequency varies as the plasma expands. When the radio frequency equals the plasma frequency, resonance occurs and resonance signal is observed. The resonance signal is due to the increased evaporation of electrons. This approach was used to model the plasma density as a function of time and also calculate the average plasma density. Kulin's study incorporated hydro dynamic model to explain plasma expansion. However, there were discrepancies in the model and the observations at low temperature and high density

because the model did not consider strong coupling of plasma at low temperature. This model also did not incorporate the fact that the electron density and thus the plasma frequency varies with position within the plasma. The plasma resonance frequency in the local mode is given by the equation $\omega_p(\mathbf{r}) = \sqrt{4\pi e^2 n(\mathbf{r})}$, where e is the charge of an electron and $n(\mathbf{r})$ is the electron density at position $\mathbf{r}$.

2.2 Quasi mode

The quasi mode is dependent on the average density of the plasma rather than the local plasma density. The quasi mode resonant frequency equals the average plasma frequency. In quasi mode, each point in plasma is resonating with the same average resonant frequency. Bergeson et al. came up with this theory in 2003 [7]. Bergeson used hydro dynamic model for cold plasmas to model the plasma expansion. This model contains a damping factor γ which incorporates the effect of inter-particle collisions and in this model plasma oscillation is modeled as forced driven oscillation. The plasma was found to have a continuous response to the radio frequency rather than the discrete response as given in the local mode of oscillation. The average plasma resonance frequency $\bar{\omega}_p$ in the quasi mode is given by $\bar{\omega}_p(\mathbf{r}) = \sqrt{4\pi e^2 \bar{n}(\mathbf{r})}$, where $\bar{n}(\mathbf{r})$ is the average plasma density. The damped quasi frequency was calculated as 0.37 $\bar{\omega_p}$. This model also underestimated the density of ultra cold plasma found using local mode analysis.

2.3 Edge Mode Resonance

One may conclude that neither the picture of local absorption nor the quasi mode permits consistent rf absorption measurements [8]. Lyubonko et al. resolved the discrepancies that provided a consistent description of the plasma oscillation [8]. The

edge mode resonance is based on the fact that experimental plasmas are quasi neutral with charge imbalance. Some electrons are lost during the creation of plasmas and the others are extracted by the externally applied electric field that is used to detect the electrons. The charge imbalance creates an outer edge of the electron density, which is consequently described by a truncated Gaussian distribution. The charged particle density at zero temperature is given by the equation

$$n(r) = n_0(r)f(r) + \delta n(r)\exp^{-i\omega t} \tag{2.3.1}$$

where $n_0(r)f(r)$ is the equilibrium density of the plasma and δn is the charge imbalance created due to the a weak external radio frequency field $\mathbf{E}\exp^{i\omega t}$ [8]. Substituting this equation into the hydro-dynamic model governing plasma expansion yields

$$\left(\frac{\omega_{p0}^2}{\omega^2 + i\omega\nu} - f(\mathbf{r})\right)\nabla^2\phi - \nabla f(\mathbf{r})\nabla\phi = -\mathbf{E}\nabla f(\mathbf{r}) \tag{2.3.2}$$

where ω_{p0} is the peak plasma frequency and the parameter ν represents the collisional damping. In this equation, the charge imbalance has been replaced by the corresponding electrostatic potential ϕ by using the equation

$$\delta n = \nabla^2\phi \tag{2.3.3}$$

Assumptions of $\mathbf{E} = 0$ and $\nu = 0$, then yields

$$\nabla(\epsilon\nabla\phi) = 0 \tag{2.3.4}$$

Equation 2.3.4 is Maxwell′s equation with dielectric function

$$\epsilon(\mathbf{r}) = 1 - \frac{\omega_{p0}^2}{\omega^2} f(\mathbf{r}) \equiv 1 - \frac{\omega_{p0}^2}{\omega^2} \tag{2.3.5}$$

Some other assumptions are made to simplify the problem. It is assumed that the electron density n_e lies within a spherically symmetric radius of R, outside which the density is zero. The equation for potential is decoupled into radial direction and angular direction. The radial potential actually represents the disturbance of angular momentum l [8]. The plasma oscillating frequency is evaluated by using the equation

$$\epsilon(r) = \left.\frac{\partial \ln \phi^{<}}{dr}\right|_{r=R} = \left.\frac{\partial ln \phi^{>}}{dr}\right|_{r=R} \tag{2.3.6}$$

where $\phi_l^{<}$ represents the electric potential inside the boundary of the sphere and $\phi_l^{>}$ represents the potential outside the boundary of the sphere. After incorporating boundary conditions and guessing the solution for $\phi_l^{<}$ and $\phi_l^{>}$, a solution for plasma resonance frequency eigenvalue for the given R is obtained [8]. The equation is solved using numerical analysis. By finding a relation between plasma edge radius and the degree of charge imbalance, a solution for plasma resonance frequency as a function of charge imbalance δ can be determined. In the experimental data a function $\delta(t)$ needs to be determined because δ is not constant, but varies with time. The number of electrons extracted by the field E_{ext} as a function of time can be determined using the equation

$$\alpha \equiv \frac{E_{ext}\epsilon_0\sigma(t)^2}{4\pi N_i} \tag{2.3.7}$$

It should be noted that E_{ext} is a small static electric field that is applied so that plasma electrons drift towards a micro-channel plate so that they can be detected. The detection electronics set up can be referred to in Section 3.1.6. The relation

between charge imbalance and the resonant frequency can be then used to determine how the resonant frequency varies with time. This model of edge mode resonance by Lyubonko et al. was also verified by using many theoretical simulations by the group. Twedt et al. also experimentally verified the theory of edge mode resonance in 2011 [9]. Their experiment showed that the charge imbalance has a significant effect on the resonant frequency. They found that the plasma oscillating frequency increases with charge imbalance. In this project, we have also used similar experimental setup to investigate how the resonant frequency changes with charge imbalance.

3 Apparatus

3.1 MOT

The Magneto-Optical Trap in our lab can trap up to $\approx 1.0 \times 10^8$ Rb-85 atoms at a nominal temperature of $\sim 100\ \mu K$ with a maximum density of $\sim 5.0 \times 10^{10}\ cm^{-3}$ [4]. The MOT contains following components.

3.1.1 Steel Chamber

The lab has a cylindrical steel chamber of radius 7.5 cm and height 30 cm. UNPs are made by photoionization of laser cooled atoms in a MOT. For the MOT to work, the atoms must be in an environment where the pressure is below 10^{-9} Torr. The combination of ordinary vacuum and ion pump is used to bring the vacuum level of the chamber to around 10^{-10} Torr. The chamber contains six windows oriented to allow laser beams to enter and exit the chamber from three different orthogonal directions. The chamber is also wrapped with two different wire coils on the top and bottom in anti-Helmholtz configuration. This anti-Helmholtz configuration varies the magnetic field inside the chamber. After completely evacuating the chamber, a rubidium finger connected to the vacuum chamber is used to introduce gases rubidium into the chamber. Heating tape wrapped around the rubidium finger is used to heat the rubidium atoms and create rubidium vapor. The rubidium vapor is then laser cooled inside the chamber and magnetically trapped. A UNP is formed from the cold atoms by photoionization using light from a pulsed dye laser.

3.1.2 Cooling Lasers

A laser with narrow bandwidth is required for laser cooling because energy levels are quantized. Narrow bandwidth lasers are generally expensive as well as not tunable.

Diode lasers offer inexpensive solution; however, they have relatively wide line width. External cavity set up helps us overcome this problem of wide line width. An external cavity diode laser (ECDL) contains a diode laser and the output of the diode laser is directed towards a diffraction grating. The grating is angled so that the first order diffraction is directed back into the cavity. This first order beam provides optical feed back to the laser diode chip. The emission wavelength can be tuned by rotating the diffraction grating. In our experiment, two ECDLs were used. The number of photons produced by ECDL is not enough to laser cool all the Rubidium atoms inside the chamber. Therefore, additional laser power is achieved by using amplifier diode lasers. The combination of the oscillator laser and the non-cavity diode amplifier laser is used to laser cool atoms in the optical chamber. Light from the oscillator laser (also called master) is sent to the amplifier laser (also called slave). This light stimulates the amplifier diode to emit at the same frequency as the oscillator diode. The light from amplifier diode is prohibited from getting back to oscillator diode by using optical isolator.

The ECDL is tuned so that its frequency (in the lab frame) is approximately 10-20 MHz lower than that at which the stationary atom will absorb. Hence, only atoms moving toward the lasers will "see" the frequency upshifted due to the relativistic Doppler shift. The frequency of the laser beam is doppler shifted by the amount $-(V/c)\nu_\sigma$ from the reference frame of Rubidium atoms. At a particular velocity, the atom will perceive the frequency be resonant, and absorb from the laser. As it does so, it receives a small momentum "kick" of an amount equal to the laser photon$'$s initial momentum. The momentum "kick" that the atom receives from each scattered photon is small, but by exciting a strong atomic transition, it is possible to scatter as many as 10^7 atoms per second and produce acceleration of 10^4 g. [10] In our experiment, the cooling laser is tuned such that the Rubidium-85 transitions from

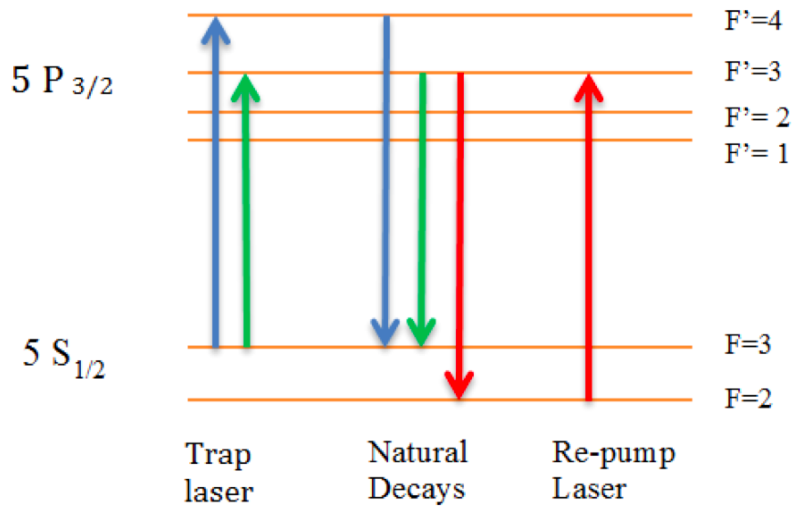

Figure 1: A schematic of the allowable excitations and decays on the Rb-85 atom. The excitation from F=3 to F′=3 is possible due to the non-zero width of the $5p_{1/2}$ hyperfine states.

the $5s_{1/2}$,F = 3 hyperfine state to the $5p_{1/2}$ F′=4 upper state. This corresponds to the wavelength of 780 nm.

Figure 1 shows the energy levels of Rb-85 atoms. We can assume that based on the selection rule all the excited atoms will end back in F = 3 state. However, there is some probability that some atoms will excite to F′=3 state from F=3 state. When this happens, the atoms might decay back to F=3 state or F=2 state. The F=2 state is also called a dark state because in this state, the cooling lasers will not be able to excite any atoms and hence the process of laser cooling stops. If we do not rectify this situation, then all the atoms might decay to F=2 lower state after certain time interval. The solution to this problem is using another laser that excites Rubidium-85 atoms from F=2 state back to F′=3 state and hence makes sure the process of laser cooling continues. The re-pumping laser has the same set up as the cooling laser. A small fraction of the light is sent to spectrum analyzer. Spectrum analyzer can be used to verify that the cooling and re-pump amplifier lasers are successfully locked to

the right frequency. We can observe the signal from both the cooling and re-pumping lasers in oscilloscope and lock them to correct frequencies. Edge-lock laser lock is used to lock the laser frequency. This arrangement of lasers to cool atoms is called "optical molasses". In this configuration, atoms are being bombarded by laser beams from all three orthogonal directions. The optical alignment of laser beams for the MOT trap is shown in figure 2 and figure 3.

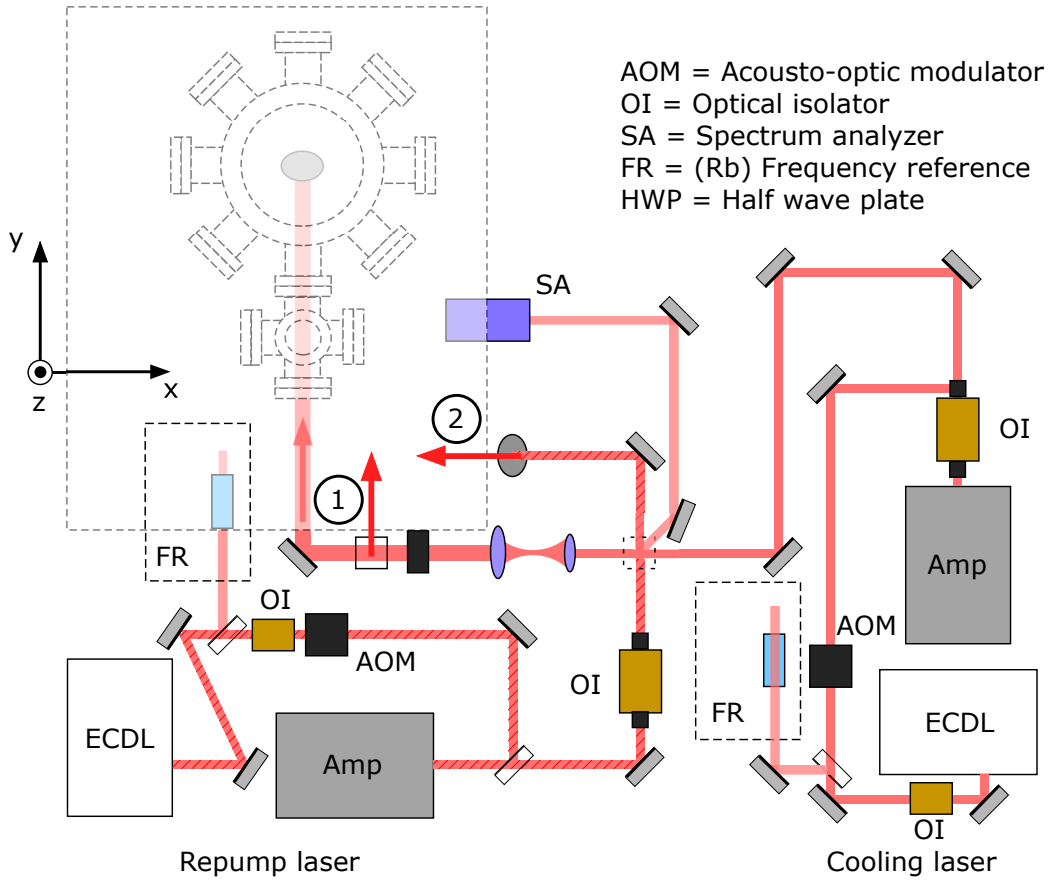

Figure 2: A schematic of the lower level of the optical apparatus used to guide the laser beams into the MOT from three orthogonal directions. At locations (1) and (2) the beam is reflected towards z-directions.[11]

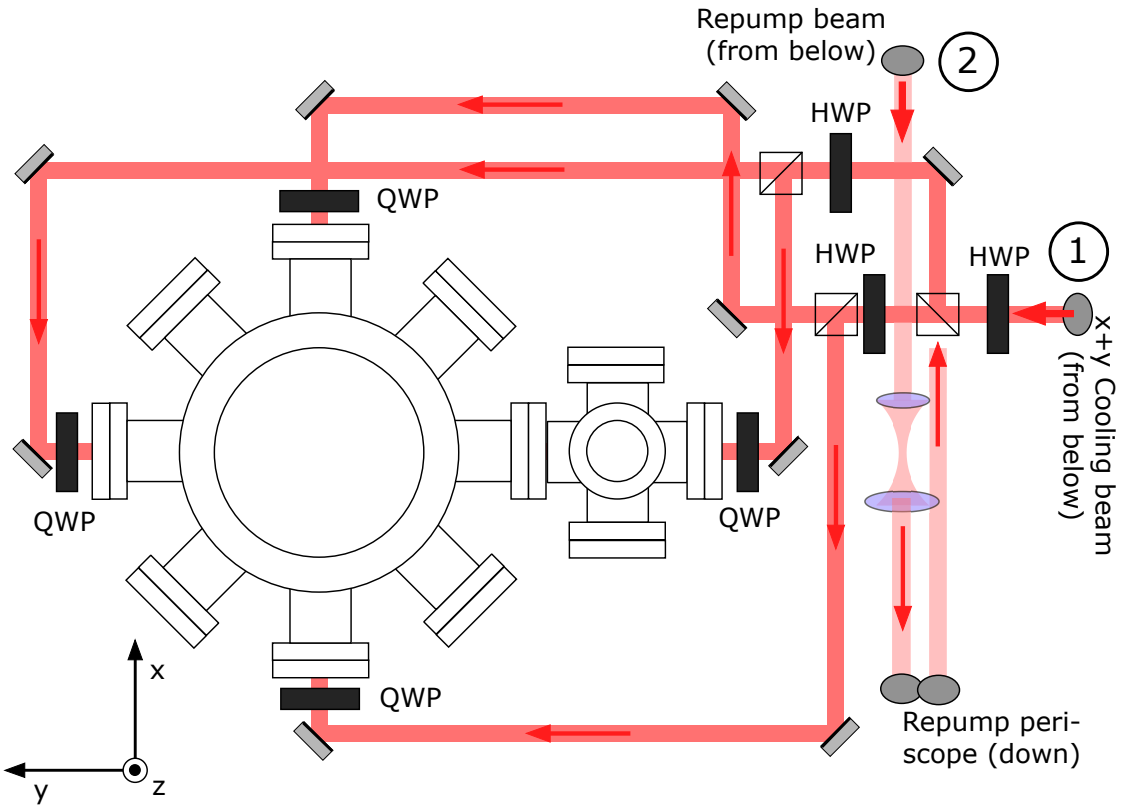

Figure 3: A schematic of the upper level of the optical apparatus used to guide the laser beams into the MOT from three orthogonal directions. At locations (1) and (2) the beam is reflected towards z-directions. [11]

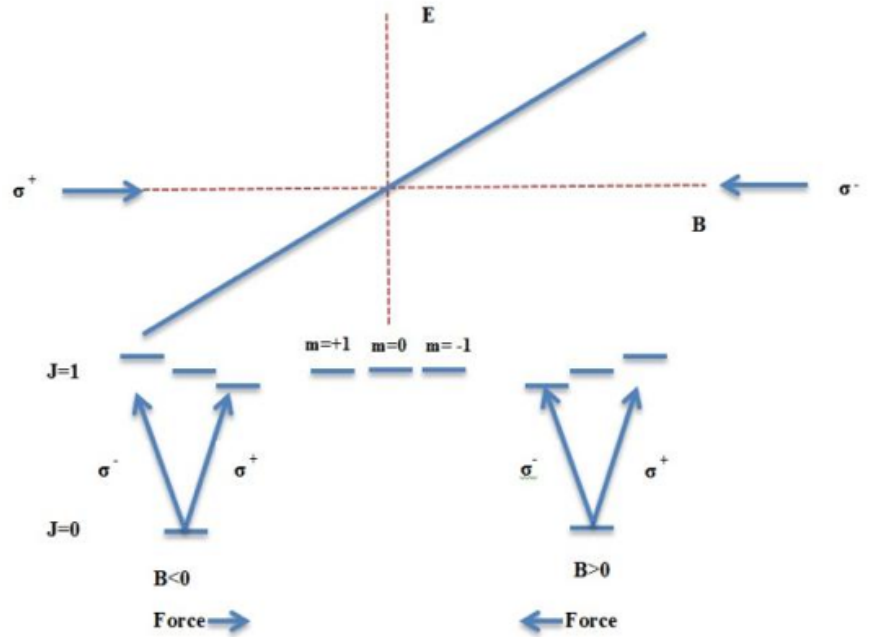

Figure 4: A schematic of the splitting of the J = 1 energy level in presence of the linearly varying magnetic field along the z-direction. The right handed polarized (σ^+) photons are absorbed by atoms moving to the left while left handed polarized (σ^-) photons are absorbed by the photons moving to the right. The net effect of the process pushes the atoms to the center.

3.1.3 Magnetic Field

The two copper coils wrapped on the top and bottom of the cylindrical steel chamber produce a linear magnetic field within the chamber in all three orthogonal directions. Each laser beam is circularly polarized using a quarter wave polarizer before entering the vacuum chamber. The beam enters the chamber with polarization in one direction, exits the chamber, gets reflected and enters back into the chamber in opposite polarization direction. These two polarization directions are denoted by σ^+ (right handed polarized) and σ^- (left handed polarized) respectively. The transition of Rb-85 atom in our experiment is from F = 3 to F$'$ = 4 state. However, let us consider a transition from F=0 to F$'$=1 state for simplicity. Let's just consider the case of z-direction.

The magnitude of the Doppler shift from the reference frame of a rubidium atom is dependent on atomic velocity. The faster an atom is moving, the lower is the frequency of the beam required to excite it. In the presence of an external magnetic field, the three energy levels m=-1,0 and 1 lose their degeneracy due to Zeeman effect as shown in the figure 4. The σ^+ laser beam causes transition from m=0 to m$'$=+1 while the σ^- causes transition from m=0 to m$'$=-1 state. The atoms moving towards the negative z-direction get excited by σ^+ laser beam because this is closer to the resonance from the Doppler shifted laser. However, the atoms moving to the positive z direction are far from frequency of σ^- laser beam. When an atom moving towards the negative z direction gets excited by the σ^+ laser beam, it slows down and gets pushed closer towards the origin. When the atom slows down, the magnitude of the Doppler shift also decreases. Therefore, the atom "sees" the photon at a slightly higher frequency from its reference frame. However, the frequency of the photons used for the laser cooling remain constant through out the experiment. This implies that the atom cannot be further slowed down because it will not absorb the photons any more. Nevertheless, the laser cooling process continues. This is because the difference between energy levels is proportional to the strength of the external magnetic field. As the atom is slowed down and gets closer to the origin, the difference in energy levels between m$'$=0, m$'$=1 and m$'$=-1 decreases as magnetic field strength decreases closer to the origin. This increases the difference in energy levels between F=0, m=0 and F$'$=0, m$'$=1 state. Therefore, the atom is still able absorb the higher frequency photon, which further slows its down. After a few absorption and emission proceses, the atom will still be in $z < 0$ region, but will be moving slower. After laser cooling the atoms, they are photo ionized by pulsed laser beam from Nd:YAG laser to form ultra cold neutral plasmas. The theory behind evolution of this plasma has already been discussed in Section 1.2.2.

3.1.4 Photoionization Laser

After laser cooling the atoms, they are ionized using a pulsed, dye-amplifier laser. The set up is based on Littman type dye laser [12]. A neodymium-doped yttrium aluminum garnet (Nd:YAG) laser, pulsed at 20 Hz, emits light at wavelength of 1064 nm. The Nd:YAG laser is operated in the Q switching mode. In this mode, the population inversion in the garnet builds up and when it is at the maximum, a light ray is allowed to go through and set off the lasing process. This lasing process depletes the population inversion buildup and the lasing process discontinues after 10 ns so that the garnet gets another opportunity to achieve a population inversion. The 1064 nm output of the Nd:YAG laser can be converted into 532 nm (second harmonic) and 355 nm (third harmonic) using non linear crystals. The 355 nm laser beam is wavelength separated from the other harmonics and is used to pump the gain medium of the Littman dye laser. The dye (lasing medium) is a circulated 1-to-10 solution of Coumarin 480 dye in methanol. As the laser beam passes through, the excited Coumarin 480 molecules are stimulated to decay and then emit photons. A double diffraction grating system is used to tune the laser output to a wide range of wavelength. This process amplifies the power of the laser to around 13 mW, which can be boosted by adding another dye cell amplifier. The upper limit of the output laser can produce electrons in the order of 200K while the lower limit of the output laser is below the ionization threshold of Rb-85 atoms.

3.1.5 Timing Electronics

The timing is shown schematically in figure 5. The photo ionizing lasers, electric field pulses pulses and detection electronics are all synchronized by externally triggered or gated pulses delayed by varying time intervals from a master digital delay

generator (DDG) [4]. The first trigger pulse is sent to Nd:YAG laser, which excites the gain medium through flash lamp pulse. A second trigger turns off the MOT magnetic field about 50 μs before firing the laser. A third trigger is sent to the laser and the oscilloscope at the same time. This third trigger directs the oscilloscope to start acquiring the data. After the plasma expansion has finished another trigger is fired to resume the normal operation of magnetic field.

The ECDL laser cools the Rb-85 atoms by exciting them from $5s_{1/2}$ to $5p_{3/2}$ state. Then a pulsed light from Littman laser is used to photo-ionize the laser cooled Rb-85 atoms. Right after the formation of plasma, there is a spike in the electron signal. This first burst of electrons represent the highly energetic electrons on the edges of plasma that acquire enough kinetic energies to completely escape the electrostatic potential inside the plasma. The ejection of these electrons leaves excess positive charge in the plasma which strongly hold the remaining electrons within the plasma. Thermal energy is released in the plasma due to the collisions between electrons and ions. The plasma then expands due to the pressure of excess ions. The expansion decreases the density of ions and hence the potential well depth of the electrons also decreases. During this process, the plasma has life time of around 10 to 100 μs. While the plasma is expanding, its density is changing. The changing density also changes the plasma oscillation frequency or frequency with which the electrons are vibrating about the stationary ions. page

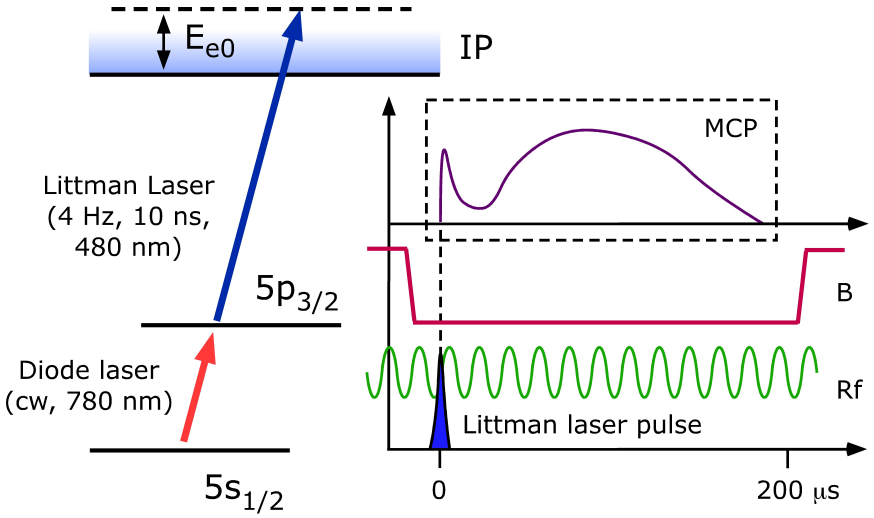

Figure 5: A schematic of the graphical summary of the experimental procedure.[11]

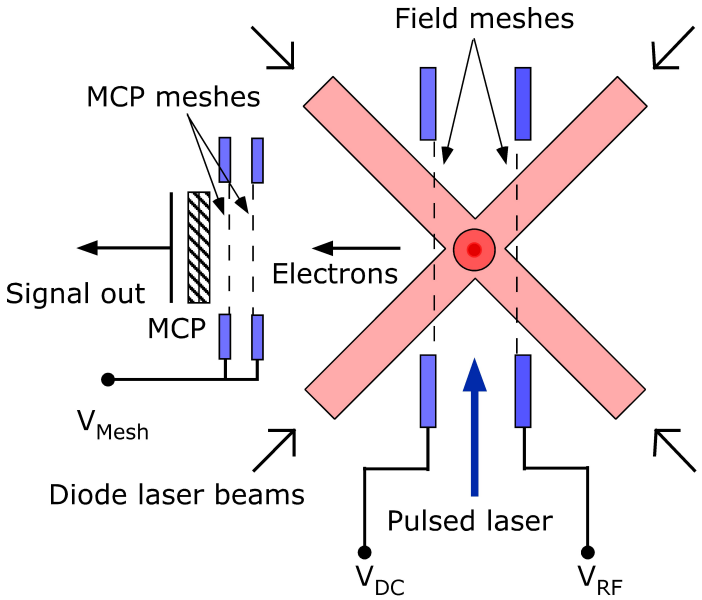

Figure 6: A schematic of the electrodes and detection setup inside the MOT [11]

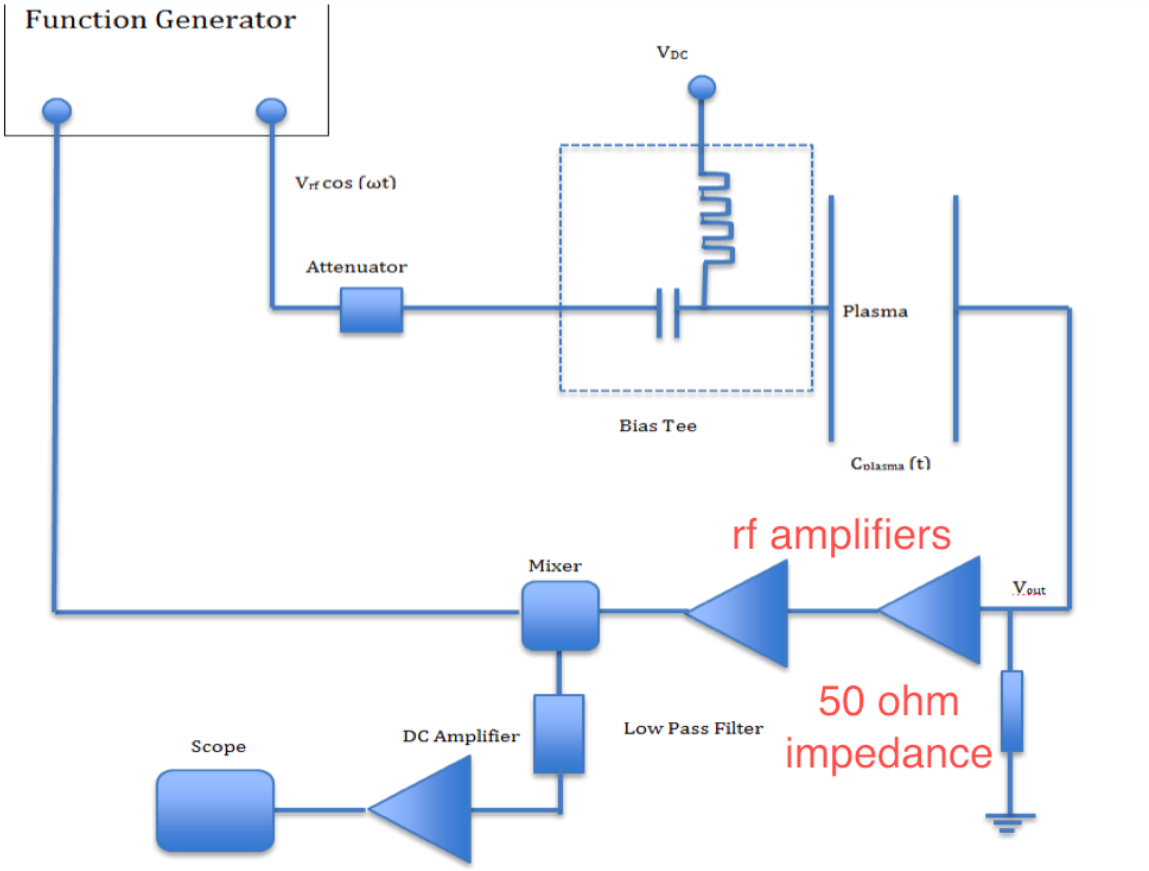

Figure 7: A schematic of the homodyne circuit used to apply radio frequency signal to the plasma.

3.1.6 Detection Electronics

The MOT chamber also contains field meshes and Micro Channel Plate (MCP) detector. Figure 6 shows the electrode setup inside the MOT. The copper field meshes are used to apply time varying radio frequency signal to the plasma in the center of the MOT. The radio frequency is generated using an arbitrary function generator. The same copper field meshes are also used to apply small electric field, E_{ext}, to accelerate the free plasma electrons towards MCP detector. The copper field meshes also push the majority of escaping electrons towards the MCP detector. The MCP signal is amplified and is acquired using a digital oscilloscope. The data from the

digital oscilloscope can be transferred to computer using a program written in Lab View.

In our experiment the plasma oscillation is driven by a weak radio frequency field. Figure 7 shows the setup for investigating the radio frequency absorption of the plasma. The homodyne circuit can be modeled as a high pass filter. The objective the apparatus is to detect the change in the amplitude and phase of the transmitted radio frequency wave that is due to the presence of the plasma. The Plasma is in between two copper field meshes and this combination is modeled as a parallel capacitor with capacitance $C(t)$. The output voltage is effectively measured across the 50 Ω input impedance of the radio frequency amplifier. The function generator is used to generate a radio frequency signal $V_0 \cos(\omega t + \phi)$. V_0, ω and ϕ are all constants that can be controlled using the function generator. A bias tee is used in the circuit to add a DC offset to the radio frequency signal, which is used to push the plasma electrons towards the MCP. The high pass filter (parallel plate capacitor controlled by the meshes plus the 50 Ω input impedance) changes the amplitude and the phase of the input signal such the output of the high pass filter becomes $\mathrm{A}V_{rf}\cos(\omega t + \theta)$. Obviously, A and θ mostly depend on the meshes and 50 Ω impedance, but a small part of each depends on the plasma. The output signal is amplified by two amplifiers, which amplify the signal by a factor of G. The initial input from the function generator and the output from the high pass filter are mixed in the mixer. The output of the mixer is passed through a low pass filter before sending the final signal to the oscilloscope.

The following equations summarize the process mathematically. The output of

the mixer is

$$\begin{aligned} V_{out} &= V_0 \cos(\omega t + \phi_0) \times GAV_{rf} \cos(\omega t + \theta) \\ &= GAV_0 V_{rf} \cos(\omega t + \phi_0) \cos(\omega t + \theta) \\ &= GAV_0 V_{rf} \left[\frac{1}{2} \cos(2\omega t + \phi_0 - \theta) + \frac{1}{2} \cos(\phi_0 - \theta) \right] \end{aligned} \tag{3.1.1}$$

The factor $\frac{1}{2}\cos(2\omega t + \phi_0 - \theta)$ in 3.1.1 is filtered out by the low pass filter in the homodyne circuit and hence the final signal that is observed in the digital oscilloscope is $\bar{V}_{out} = \frac{1}{2} GAV_0 V_{rf} \cos(\phi_0 - \theta)$. The low pass filter averages V_{out} in equation 3.1.1.

Equation 2.3.5 relates the permittivity $\epsilon(t)$ of the plasma to the plasma oscillation. The permittivity $\epsilon(t)$ of the plasma can also be related to the gain A and phase θ of the homodyne circuit. The capacitance of flat metallic plates of area S and plate separation d is given by the following equations.

$$\begin{aligned} C_{vacuum} &= \epsilon_0 \frac{S}{d} \\ C_{plasma}(t) &= \epsilon(t) C_{vacuum} \\ &= \epsilon(t) \epsilon_0 \frac{S}{d} \end{aligned} \tag{3.1.2}$$

For a high pass filter the gain A is given by

$$A = \frac{1}{\sqrt{\left(1 + \left(\frac{1}{\omega C_{plasma} R}\right)^2\right)}} = \frac{1}{\sqrt{\left(1 + \left(\frac{1}{\omega \epsilon(t) \epsilon_0 \frac{S}{d} R}\right)^2\right)}} \tag{3.1.3}$$

The phase shift θ is given by

$$\theta = \tan^{-1}\left(\frac{1}{\omega R C_{plasma}}\right) = \tan^{-1}\left(\frac{1}{\omega R \epsilon(t) \epsilon_0 \frac{S}{d}}\right) \tag{3.1.4}$$

Both the amplitude change and the phase change signals from the mixer are sent to the digital oscilloscope. The analysis of the radio frequency phase change and amplitude change signals play crucial role in determining $\epsilon(t)$ and hence the resonant frequency ω_p.

4 Results

Figure 8 shows a plot of the electron signal during plasma expansion for the radio frequency of 8 MHz. The profile of the signal closely resembles what would be expected for plasma evolution. Right after the photoionization process, there is a spike indicating the first burst of electron ejection. The spike arises due to several factors. First the photo-ionizing laser ejects the electrons and there are some electrons, especially on the edges, that have enough energy to escape the plasma. The number of electrons ejected initially can be controlled by changing the intensity of photo-ionizing laser. Moreover, disorder induced heating and three body recombination process also heat the plasma. Some electrons acquire enough kinetic energies from the heat energy generated from these two heating processes to completely leave the plasma. Then, the electron signal gradually decreases again to a very low level at around 20 μs. This is the situation where the excess positive charge is strongly holding the remaining electrons within the plasma. The plasma starts expanding due to the increased ion pressure. As plasma expands, the electrostatic potential wells start getting shallower. As a consequence, more electrons start leaving the plasma and this can be observed in the gradual increase in the electron signal again. As plasma expands, more electrons leave the plasma.

By 100 μs, almost all the electrons leave plasma and the plasma's life ends. The figure 8 has two profiles. The curves in these two profiles start separating at around 25 μ s. The UNP in the upper curve has a shorter lifetime than the lower curve. This is because the curve on bottom is the plasma signal when the radio frequency is not applied while the curve on the top is the plasma signal when the radio frequency is applied. The radio frequency signal excites the plasma during the resonance causing enhanced ejection of the electrons. Due to this enhanced ejection of electrons the

plasma life ends earlier than it would have ended had the radio frequency not been applied.

The resonance peak can also be observed using the radio frequency absorption signal as shown in the figure 9. There is a sudden dip in the amplitude signal at around 42 μs. This dip corresponds to the resonance. There is an enhanced electron ejection at this point. This can be observed in the spike in the electron signal in figure 8. This is also seen in the spike in the black curve at the same time in 9. The black curve is the difference in the electron evaporation signal with and with out external radio frequency. The radio frequency absorption was also performed with various frequencies of the radio frequency field. It was observed that as the external driving frequency is increased the resonance peak is observed earlier in time during the plasma expansion. Figure 10 shows how the time of the electron resonance varies with the frequency of the radio frequency. As the plasma expands, its average density is decreasing and hence the electron oscillation frequency is also decreasing. Therefore, resonance occurs later in time for the lower radio frequency.

In addition, the degree of charge imbalance, δ, in the plasma increases from almost zero early in the UNP evolution, to 1 at the end. A higher degree of change imbalance is associated with stronger radio frequency absorption at the edge mode in Lyubonko et al.'s model [8]. The radio frequency absorption does appear to be stronger at 3.5 MHz than at 10 MHz, but the absorption is quite strong over a large fraction of the UNP lifetime, which is not what is expected for the behavior of the edge mode.

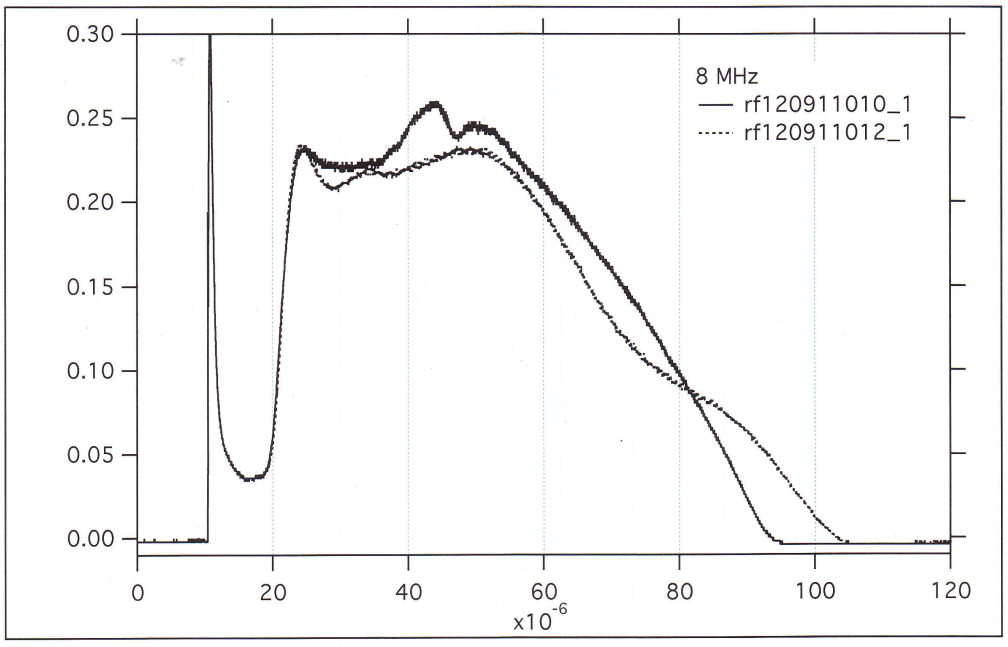

Figure 8: The MCP detector signal from the plasma as observed in the oscilloscopeThe curve on the top corresponds to plasma signal without radio frequency while the curve on the bottom corresponds to plasma signal after applying the radio frequency. The frequency of the input voltage signal was 8 MHz.

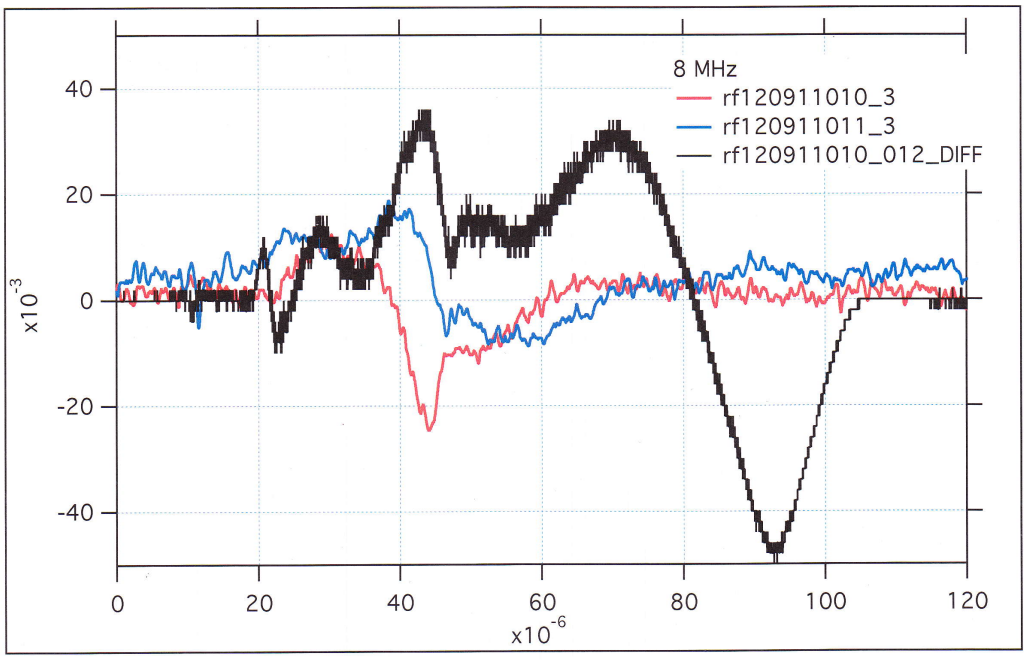

Figure 9: The radio frequency gain change signal (red) and the radio frequency phase signal (blue) from the homodyne circuit. The resonance can be observed at around 42 μs as there is a dip in the rf amplitude signal. The dark curve corresponds to the difference in electron signals with and without radio frequency from figure 8.

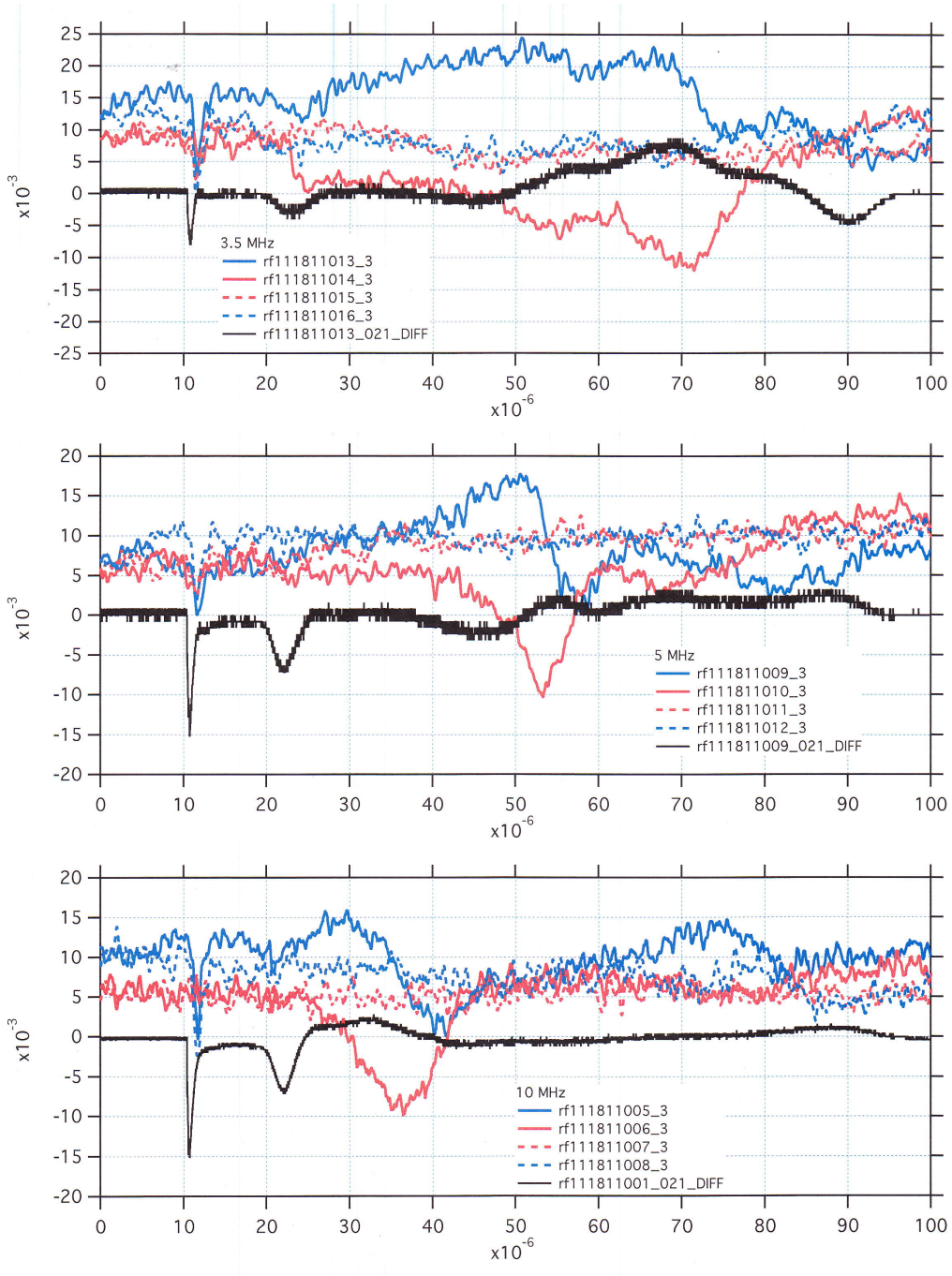

Figure 10: The rf amplitude change (red) and phase change signals at applied frequencies of 3.5 MHz, 5 MHz and 10 MHz. As can be clearly observed the resonance occurs earlier in time as the frequency is increased. The dotted plot corresponds to the rf amplitude change and phase change signals without the plasma. The black curve is the difference between the electron signals with and without the radio frequency signal

5 Conclusion

The experimental results are in good qualitative agreement with theoretical model proposed by Lyubonko et al. and experiments performed by Twedt et al. Enough data have been collected for quantitative analysis. In the future, quantitative analysis will play an important role in verifying the results with the edge-mode theory. The quantitative analysis will also lead to the determination of the accurate actual value of the resonant frequency ω_{p0}. The charge imbalance can then be evaluated by integrating the MCP electron signal from the beginning to the point at which the resonance occurs. Then a plot of ω_{p0}. vs δ can be made to verify the edge mode theory. To evaluate the value ω_{p0}, we need to quantitatively analyze the amplitude and phase shift change signals. The signals right now have relatively low signal to noise ratio. This will lead to some inaccuracies in the determination of the value of ω_{p0}. Therefore, some steps should be taken to filter the noises from the amplitude absorption signal. The parameter δ can be varied using voltage pulses of various time interval and magnitude. Once the value of ω_{p0} can be determined accurately, various plasma parameters like plasma expansion velocity, plasma temperature and density can also be determined accurately . The future experiments and analysis can also be used to check the consistency and reproducibility of the UNP experiments.

References

[1] S. L. Rolston. Ultracold Neutral Plasma. *Physics*, 1(2), (2008).

[2] S. D. Bergeson L. A. Orozco C. Orzel T. C. Killian, S. Kulin and S. L. Rolston. *Physical Review Letters*, 83(4776), (1999).

[3] T.C. Killian, T. Pattard, T.Pohl and J.M. Rost. Ultra Cold Neutral Plasmas. *Physics Reports*, 449:p. 77–130, (2007).

[4] D.A. Tate. *Rydberg Atoms and Their Effect on Ultra-cold Plasma Dynamics.* Colby College, (2011).

[5] R.S. Fletcher. Three-body Recombination and Rydberg Atoms in Ultracold Plasmas. *Department of Physics, University of Maryland.*

[6] S. Kulin, T.C. Killian, S.D. Bergeson, and S.L. Rolston. Plasma Oscillations and Expansion of an Ultracold Neutral Plasma. *Physical Review Letters*, 85(2), (2000).

[7] S.D. Bergeson and R.L. Spencer. Neutral-plasma Oscillations at Zero Temperature. *Physical Review*, E.67(026414), (2003).

[8] A Lyubonko, T Pohl, and J.M. Rost. Energy Absorption of Quasineutral Plasmas Through Edge-modes. arXiv: 1011.5937v1 [Physics of Plasmas], (2010).

[9] K.A. Twedt and S.L. Rolston. Electronic Detection of Collective Modes of an Ultracold Plasma. *Physics of Plasmas*, 108(065003), (2012).

[10] C. Wieman, G. Flowers and S. Gilbert. Inexpensive Laser Cooling and Trapping Experiment for Undergaruate Laboratories. *American Association of Physics Teachers*, 63(4), (1995).

[11] D.A. Tate. *Figures Provided by Professor Tate.* Colby College, (2011).

[12] M.G. Littman and H.J. Metcalf. Electronic Spectrally Narrow Pulsed Dye Lasers Without Beam Expander. *Applied Optics*, 17(14):p. 224–227, (1978).